Inorganic Chemistry

Article

pubs.acs.org/IC

The Structure of *MLn(hfbc)$_4$* and a Key to High Circularly Polarized Luminescence

Sebastiano Di Pietro and Lorenzo Di Bari*

Dipartimento di Chimica e Chimica Industriale, Via Risorgimento 35, 56126 Pisa, Italy

Supporting Information

ABSTRACT: The heterobimetallic complex *CsEu[(+)-hfbc]$_4$* (*hfbc* = 3-heptafluorobutyryl camphorate), prepared by Kaizaki and co-workers, displays the highest ratio of polarization versus total luminescence (measured by the g_{lum} factor), i.e., ∼85% of the emitted photons at 595 nm are left-circularly polarized. We present a detailed structural analysis in solution, based on paramagnetic nuclear magnetic resonance (NMR), and discuss the possible dynamic processes, where its analogues are involved. We demonstrate that the first coordination sphere is very close to the achiral regular square antiprism (SAPR) with D_{4d} symmetry, which rules out the intrinsic dissymmetry of the Eu environment for rationalizing the g_{lum}. In contrast, the dynamic coupling between the *f*–*f* transitions, responsible for the emission, to the ligand-centered π–π^* transition at 310 nm displays almost ideal geometry to justify g_{lum} and discloses a key to high circularly polarized emission.

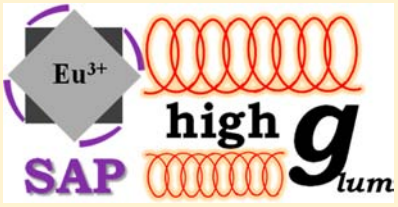

INTRODUCTION

Circularly polarized luminescence (CPL) has recently received larger interest and, after decades where the bases were thrust but one would find only niche applications, it now appears to be a promising and emerging chiroptical technique.[1−4]

There are at least two physical parameters that characterize a good compound for CPL: a strong total luminescence (measured by the quantum yield) and a marked difference in the intensity of left- and right-circularly polarized emitted radiation, as conveniently measured through the dissymmetry factor, g_{lum}:

$$g_{lum} = \frac{2(I_L - I_R)}{I_L + I_R} \quad (1)$$

where I_R and I_L are, respectively, the intensity of the emitted right- and left-circularly polarized light. Lanthanide complexes display very interesting properties in this context, because they emit light in very well-defined spectral regions, very often with extremely narrow bandwidths, reminiscent of atomic spectra, and, because of the symmetry properties of the electronic transitions responsible for this process, they may display high g_{lum} values.[5] To the best of our knowledge, the record compound to date in this context is *CsEu[(+)-hfbc]$_4$* (*hfbc* = 3-heptafluorobutyryl camphorate, Chart 1), which, in chloroform solution, displays a value of g_{lum}(595 nm) = +1.38, which is very near to the maximum theoretical value of 2 (absolute value), corresponding to a complete polarization of the emitted bright red-orange light.[6,7] None of the closely related compounds involving the other alkali metals (Na, K, Rb) equals this record. In contrast, *CsSm[(+)-hfbc]$_4$* also exhibits extraordinarily high dissymmetry factors: g_{lum}(553 nm) = −1.15 and g_{lum}(598 nm) = +1.15.[7]

To understand the fundamental parameters responsible for the success of *CsEu(hfbc)$_4$*, it is necessary to have a precise knowledge of its geometry in *solution*, where the measurement is carried out. The available crystallographic data are insufficient to this end,[8−10] because it is well-known that lanthanide complexes very often undergo profound structural modifications upon dissolution. In contrast, paramagnetic NMR in solution gives access to accurate geometrical parameters and can reveal, characterize, and quantify dynamic processes, especially for lanthanide complexes.[11−13]

Taking advantage of our long experience in interpreting paramagnetic spectra of chiral lanthanide complexes and in relating them to their chiroptical properties,[14] we decided to investigate several elements of the series of *MLn(hfbc)$_4$* in solution. We derived an accurate solution geometry for

Chart 1. Chemical Structure of the *MLn[(+)-hfbc]$_4$* Complexes with the Labels Used in the NMR Characterization

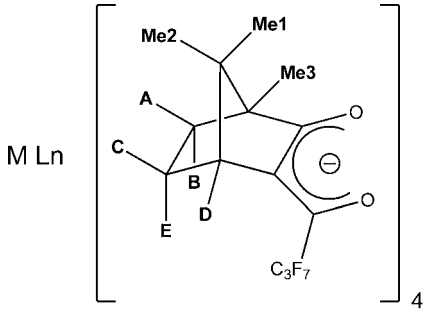

M = Na, K, Rb, Cs

Ln = La, Pr, Eu, Gd, Tb, Dy, Er, Tm, Yb, Lu

Received: August 30, 2012
Published: October 24, 2012

CsEu(hfbc)$_4$ and characterized a set of equilibria that occur as a function of solvent composition and we relate this information to the chiroptical properties of these compounds and ultimately to their CPL.

RESULTS

Solution Structure of the Cesium Derivative. All the *CsLn* derivatives (Chart 1) show proton NMR spectra ($CDCl_3$) with eight (relatively) narrow resonances, which indicates a *static* C_4 complex symmetry (v.i.).[15] [For the sake of simplicity, from this point forward, we shall refer to the complexes by specifying only the alkali metal and the lanthanide and, where it is required, the absolute configuration of the ligand (e.g., *CsEu(+)* will be used to represent CsEu[(+)-hfbc]$_4$).] The X-ray diffraction (XRD) structure reported in refs 8 and 10 lacks any symmetry and appears to be poorly representative of the solution one.

The diamagnetic ^{1}H and ^{13}C spectra of *CsLu* were assigned with standard correlation techniques; for *CsYb*, we took advantage of the known relationships between δ and T_1 parameters with structural geometrical features.[16] This led us to the assignment of the ^{1}H spectrum shown in Table 1 and Figure 1. Further homocorrelation and heterocorrelation experiments confirmed this assignment and provided ^{13}C shifts. Thanks to axial symmetry and assuming isostructurality and constant crystal field parameters, one may predict the pseudocontact shift (PCS) of any paramagnetic *CsLn* compound from the assignment of just one.[17] Thereafter, a gross estimation (temporarily neglecting the Fermi contact shift (FC), which will be introduced later) of the total shift for each proton in an unknown Ln complex can be obtained by adding the appropriate value of δ^{dia}, taken from the *CsLu* compound. Using this guide, and taking advantage of the presence of the methyl groups, which provide easily recognized singlets, we could assign the other *CsLn* proton spectra (Ln ≠ La, Pm, Sm, Gd), as reported in Table S1 in the Supporting Information.

Table 1. *CsYb* NMR ^{1}H and ^{13}C Experimental Shifts and Longitudinal Relaxation Times: Proton Pseudocontact and Fermi Contact Shifts

	Chemical Shift (ppm, $CDCl_3$)				
Position	δ^{1H}	δ^{13C}	Longitudinal Relaxation Times, T_1 (ms)	PCS[a] (ppm)	FC[b] (ppm)
Me1	−10.87	8.27	24	−12.07	−0.11
Me2	−4.70	11.60	181	−5.51	−0.04
Me3	17.68	ND	17.7	17.01	−0.05
A	−8.83	8.97	83	−10.18	0.06
B	−25.09	8.97	23	−26.09	−0.03
C	−10.37	9.04	133	−12.26	0.01
D	−17.20	18.10	76	−19.87	0.06
E	−19.92	9.04	54	−20.99	−0.04

[a]PCS = pseudo-contact shift. Evaluated using our "all lanthanides" methodology.[17] [b]FC = Fermi contact shift. Evaluated using our "all lanthanides" methodology.[17]

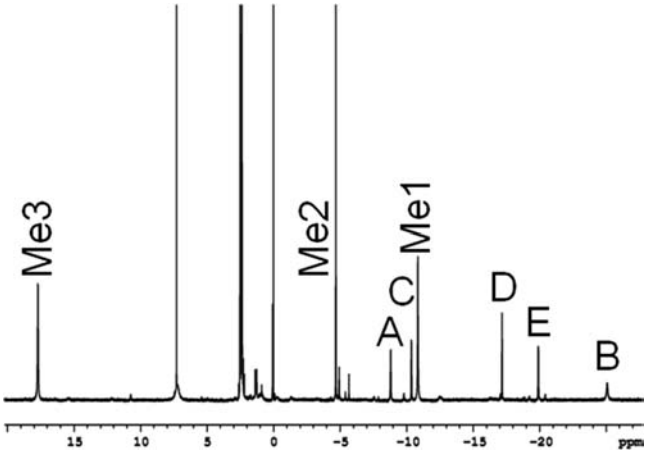

Figure 1. ^{1}H NMR spectrum of *CsYb* (600 MHz, $CDCl_3$).

In addition, we must add the diamagnetic term (a reasonable estimate is $\Delta\nu^{dia}$ = 1 Hz). Moreover, we must consider that both signals are highly structured, due to *J*-couplings: the largest splitting for proton B is 13 Hz (due to a *gem* coupling), while for proton D, it is 7 Hz. Summing all these terms, we obtain $\Delta\nu^{calc}$ = 27 and 14 Hz for E and D, respectively, which compare extremely well with the experimental values and rules out any broadening due to chemical exchange. Noteworthy, there is no trace of *cis*–*trans* isomerism, which is due to the fact that the perfluoroalkyl chains are engaged in binding the alkali metal M and must all lie on the same side of the complex.

The absence of any major dynamic structural rearrangement is demonstrated by a simple quantitative assessment, based on ^{1}H linewidths ($\Delta\nu$). Protons E and D (Chart 1) display $\Delta\nu^{exp}$ = 26 and 15 Hz, respectively. Following Table 1 and related equations in ref 14, and taking the distances from Yb of 5.3 and 5.7 Å, respectively, we can calculate paramagnetic contributions to the linewidth $\Delta\nu^{calc,para}$ = 13 and 6 Hz. To these values, we must add the diamagnetic term (a reasonable estimate is $\Delta\nu^{dia}$ = 1 Hz). Moreover, we must consider that both signals are highly structured, due to *J*-couplings: the largest splitting for proton B is 13 Hz (due to a *gem* coupling), while for proton D, it is 7 Hz. Summing all these terms, we obtain $\Delta\nu^{calc}$ = 27 and 14 Hz for E and D, respectively, which compare extremely well with the experimental values and rules out any broadening due to chemical exchange. Noteworthy, there is no trace of *cis*–*trans* isomerism, which is due to the fact that the perfluoroalkyl chains are engaged in binding the alkali metal M and must all lie on the same side of the complex.

In order to demonstrate the isostructurality of the system along the lanthanide series and to validate the assignment, we plotted δ^{para}_{Ln} vs δ^{para}_{Yb} (as reference compound), obtaining almost-perfect linear trends for Supporting Information all the investigated paramagnetic *CsLn* compounds (R > 0.99 in all cases; see Figure S1 in the Supporting Information). Starting from the slopes (m_{Ln}) of the δ^{para}_{Ln} vs δ^{para}_{Yb}, we can achieve the PCS/FC (pseudocontact/Fermi contact shifts) separation using our recently developed modified Reilley procedure.[17] The δ^{para}/S_z vs m/S_z plot (Figure S2 in the Supporting Information) gave excellent results (R > 0.99 in all cases) and the complete PCS/FC separation is reported in Table S2 in the Supporting Information and in Table 1 for the *CsYb* complex.

We may observe that the m slopes are proportional to Bleaney's C_J constants (see Figure S3 in the Supporting Information), without breaks along the lanthanide series: this means that the *CsLn* systems do not display any major crystal field parameter variation, i.e., there is no apparent coordination number variation along the series.[17]

The next step is to use the PCS values extracted from the total paramagnetic contribution to evaluate the solution structure through the routine PERSEUS:[14,18] the result for the *CsYb* derivative is reported in Figure 2, with two views, along and perpendicular to the C_4 symmetry axis. The assignment of the fluoroalkyl chains in a paramagnetic derivative (except for the CF_3 group) is not trivial, and we could not include them in the calculation.

A relevant geometrical parameter of this structure is the bite angle, which is defined as the *trans* O–Yb–O bond angle, which is 101.3°, and provides an indication that the lanthanide is very poorly accessible to axial ligands.[19] For comparison, we

dx.doi.org/10.1021/ic3018979 | *Inorg. Chem.* 2012, 51, 12007–12014

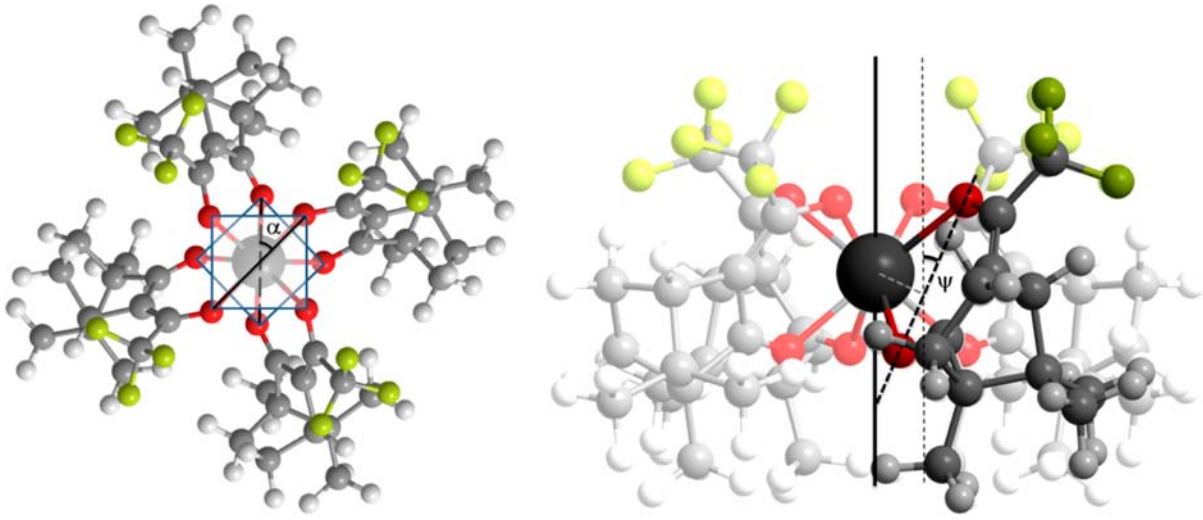

Figure 2. Solution ($CDCl_3$) structure of *CsYb* in two different views: along (left) and perpendicular (right) to the C_4 axis. The perfluoropropyl chains could not be used in the calculation, as explained in the text, and they have been represented here as trifluoromethyl groups only for a more effective visual recognition, without any structural optimization.

recall that the TSAP isomer of Yb DOTA displays a value of 133° and, for late lanthanides, it is noncoordinated to water.[20] This can be taken as a first indication of the poor propensity of *CsLn* compounds to bind axially to water or other ligands (v.i.).

A very remarkable aspect of this geometry is that the twist angle (α) between the upper and lower squares (see Figure 2) in the coordination polyhedron is −41.4°, indicating an almost-perfect square antiprism (SAPR): this means that the first sphere around Ln^{3+} is practically achiral for all *CsLn* complexes, a fact which will be the object of our discussion below. A final important geometrical feature of this structure is the ψ angle between the C_4 axis and the diketonate plane, which is equal to −27.5°, which will also be used later.

In Tables S3 and S4 in the Supporting Information, we report the details of the PERSEUS output with the differences between the experimental values and the calculated values, in order to testify the quality of the results (using Table S3 in the Supporting Information for the shifts and Table S4 in the Supporting Informationfor the relaxation rates). The agreement factor, which is defined as

$$\mathrm{AF}\,(\%) = \sqrt{\frac{\sum_i (x_{i,\mathrm{calc}} - x_{i,\mathrm{exp}})^2}{\sum_i x_{i,\mathrm{exp}}{}^2}} \times 100$$

of this structure is extremely good (below 8%, using both proton and carbon resonances).

Any other structure in solution, e.g., DD-D_2 or DD-D_{2d}, must be excluded for all elements of the series *CsLn* in $CDCl_3$.[8]

Solution Study Varying the Alkali-Metal Counterion. *NMR.* It has been known for a long time that, upon dissolution, *tetrakis* Ln camphorates can undergo the dissociative equilibrium of eq 2.[21]

$$M^+[\mathrm{ln}\ L_4]^- \rightleftarrows \mathrm{ln}\ L_3 + M^+L^-\downarrow \qquad (2)$$

The K_{eq} value is primarily determined by:

- the intrinsic stability of the *tetrakis* species $M^+[LnL_4]^-$ (dependent solely on the alkali metal and only weakly on the lanthanide ion);
- the stability and the speciation of the *tris* compound LnL_3;
- the solubility of M^+L^- in chloroform (or the solvent used).

We have seen above that axial ligation is inhibited in all *CsLn(hfbc)*$_4$, because of the small bite angle, and we may reasonably generalize this observation to all *MLn(hfbc)*$_4$. In contrast, it surely occurs for *Ln(hfbc)*$_3$: among this series of compounds, there are several well-known NMR chiral shift reagents, which is a property due exactly to their ability to (reversibly) bind organic molecules containing donor atoms.[22,23] Consequently, in eq 2, LnL_3 must be intended as a collection of species differing for the axial site occupancy, depending on solvent nature and composition. The solubility of *M*$^+$*hfbc*$^-$ in apolar solvent increases with the ionic radius of *M*$^+$. In fact, we observed that, starting from perfectly clear chloroform or dichloromethane solutions, in the course of several minutes or hours, there is the formation of a white precipitate, the abundance of which is ranked in the following order: Na > K > Rb. For Cs, the solutions never showed any decomposition.

One obtains a clear picture of the solution equilibria, by means of ^{19}F NMR of the CF_3 signal ($CDCl_3$) of the *MEu* derivatives and of commercial *Eu(hfbc)*$_3$, shown in Figure 3.

We identified the *tetrakis* (−81.9 ppm) and *tris* (−82.2 ppm) species as the major signals of the *CsEu(hfbc)*$_4$ and of the commercial *Eu(hfbc)*$_3$, respectively. In both spectra, there is a smaller signal at −80.2 ppm, which can be assigned to the free *hfbc* ligand. This latter one is present in all spectra, as a sharp line (the *J*-multiplet is not resolved) exactly at the same shift, and witnesses a certain degree of decomposition in all of the samples, including the commercial one.

The CF_3 signal for the *tetrakis* complexes moves high-field, from Na to Cs (*NaEu* = −80.89, *KEu* = −80.92, *RbEu* = −81.39 ppm, *CsEu* = −81.92 ppm), possibly due to the increasing electron density on CF_3. The time evolution of these solutions is apparent: *NaEu(hfbc)*$_4$ practically disappeared within ∼3 h, leading to a mixture of the *tris* complex and of the solid precipitate of *Na*$^+$*hfbc*$^-$ (the signal of free ligand is constant, because it is leveled by solubility product); K and Rb follow a similar fate much more slowly, while Cs remains constant.

dx.doi.org/10.1021/ic3018979 | *Inorg. Chem.* 2012, 51, 12007−12014

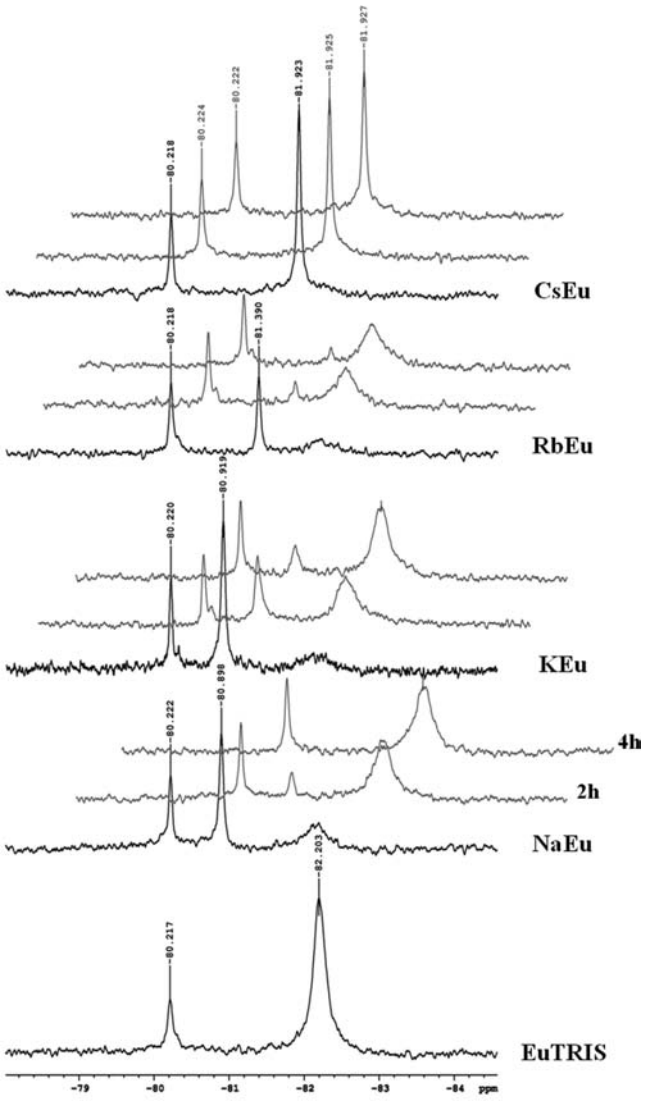

Figure 3. ^{19}F NMR ($CDCl_3$, 3 mM) spectra (particular) of the *MEu* system (M = Na, K, Rb, and Cs) and of the $Eu(hfbc)_3$. All the chemical shifts are referred to $CFCl_3$ as an external standard.

The signal of $Eu(hfbc)_3$ appears variably broadened and slightly shifted in the different samples (or at different times), because of the dynamic equilibrium at the axial position[17] and because of *cis*−*trans* (*fac-mer*) isomerism.

Inspection of the ^1H NMR spectra of the *hfbc* system in $CDCl_3$ for Na, K, and Rb confirms the dynamic process just outlined: noteworthy, in Na and K derivatives for several terms of the lanthanide series, the proton spectra show the contemporary presence of a broad paramagnetic set of resonances and a narrow paramagnetic set of resonances, which we ascribed respectively to the *tris* and *tetrakis* complexes, in slow exchange on the NMR time scale. The ^1H spectrum of *RbYb* is particularly illustrative, because it features the coexistence of a set of sharp signals at identical shifts as *CsLn,* and a set of very broad ones at completely different shifts. Interestingly, by adding of Cs^+ (CsCl) to a sample of *NaYb* (see Figure S4 in the Supporting Information), we observe the emergence of the sharp signals of the *tetrakis CsYb*. [This *NaYb* spectrum features a set of broad resonances mixed with sharp peaks. These latter ones are clustered in patterns of three signals around each shift of the tetrakis species, as if they were due to three very similar structures non- (or extremely slowly) exchanging. At the moment we are not able to provide a convincing explanation of this phenomenon.] This demonstrates the thermodynamic preference for *CsLn*, in solution, with respect to the other alkali metals. [Apparently, *CsLn* represents an energy minimum, with respect to the other MLn, and the Cs ion perfectly fits in the structure as a keystone in a vault, which is also in agreement with the findings of ref 9. In the *MPr* samples (*M* = K, Rb), we can observe that the residual water is strongly shifted upfield, as a proof that water is axially bonded (and in fast free/bound exchange) to the *tris* complex $Pr(hfbc)_3$. Moreover, at room temperature, for the praseodimium complexes, we can observe only one set of broad signals due to a fast/intermediate exchange between *tetrakis* and *tris* forms (the latter ones with further *cis*/*trans* isomerism): low-temperature experiments for the *RbPr* complex show decoalescence of the proton resonances.

(1) the smaller value of the magnetic susceptibility D for this ion makes the requisite for fast exchange less stringent than e.g. Yb;[12,13]

(2) it is not unusual that early lanthanides display faster ligand exchange rates than the late elements.

One final remark concerns the shift of water resonance. While in all the *CsLn* ^1H spectra, the water signal is around the usual value of 1.5 ppm, for all the samples obtained from the other alkali-metal compounds, δ_{H_2O} is strongly shifted upfield or downfield, according to the sign of D_{Ln} and, ultimately, the sign of C_J. [For example, Pr induces a lowfield, while Yb a strong upfield shift.] This is a further proof that water is axially bonded to the lanthanide, which is possible only for the *tris* complex, generated from the decomposition described in eq 2.

Electronic Circular Dichroism in the Ultraviolet (UV) Range. What we have observed in the NMR experiments can enlighten the interpretation of electronic circular dichroism (ECD) experiments in the UV, which provides a completely independent viewpoint on the systems and, unlike NMR, is a *fast* technique (i.e., it is insensitive to exchange rates).

The ligand-centered ECD (LC-ECD) in these complexes is largely, but not solely, determined by the exciton coupling between the $\pi-\pi^*$ transitions of the camphorate chromophores ($\lambda_{max} \approx 310$ nm), with electric transition dipole moment polarized along the diketonate O−O direction. The three most relevant parameters of the LC−ECD are (1) the couplet amplitude (difference in intensity between peak and trough); (2) the Davydov splitting (wavelength difference between peak and trough); (3) the crossover point (where CD becomes zero); and (4) the couplet asymmetry (difference in the integral of the positive and negative bands).

Before attempting any speculation on the role of exciton coupling, one must ascertain the role of *intrinsic* camphorate ECD. It consists of a broad (half width at half-maximum = 30 nm) positive Cotton effect at ~310 nm, which is superimposed to all features arising from through-space interactions between chromophores and contributes to couplet asymmetry.

The four parameters above are sensitive to the angle between the transition dipole moments and ultimately to the mutual orientations of the lines joining the two O atoms on each diketonate moiety.[24]

Focusing again on the *MEu(+)* complexes, we recorded the solution ECD spectra on 3 mM solutions (Figure 4) in different solvents: chloroform stabilized with amylene, chloroform

dx.doi.org/10.1021/ic3018979 | *Inorg. Chem.* 2012, 51, 12007−12014

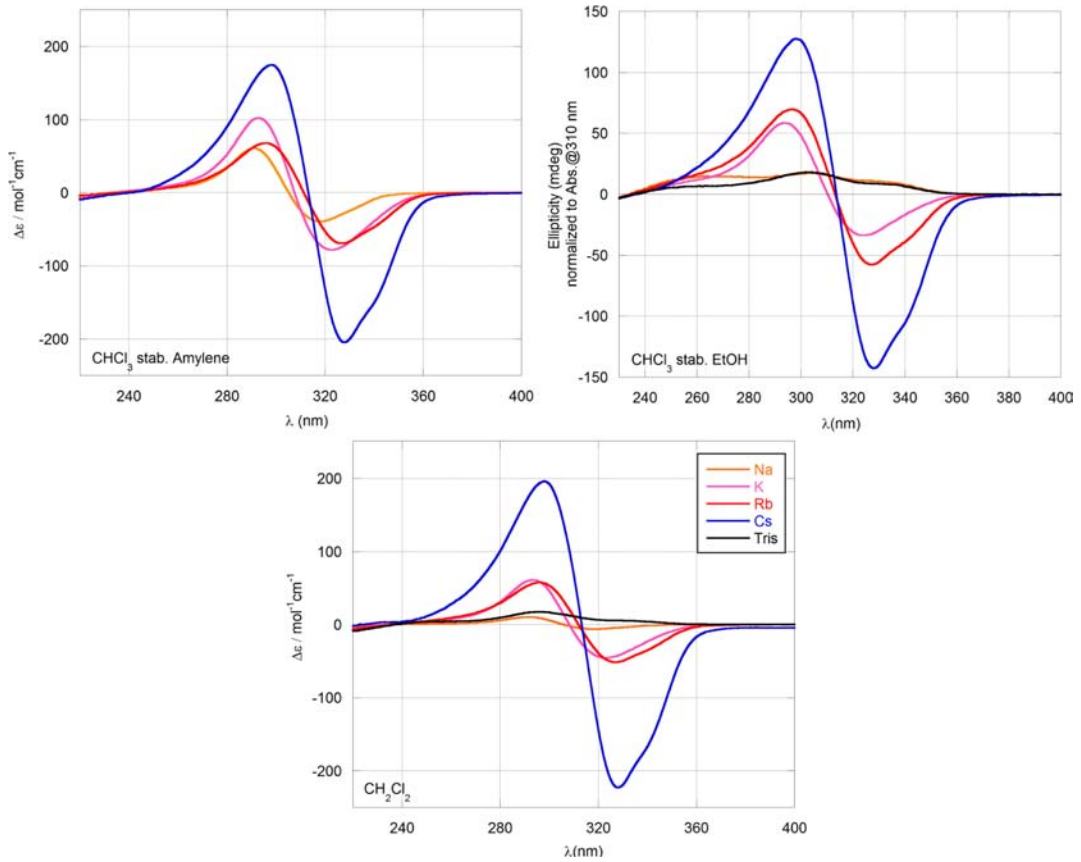

Figure 4. ECD spectra of *MEu(+)* complexes. We use the term "Tris" to indicate commercial $Eu(hfbc)_3$.

stabilized with ethanol, and dichloromethane. We made a few key observations:

- The presence of ethanol, the most common $CHCl_3$ stabilizer (~0.5%−1%, v/v), deeply perturbs the equilibrium mixture, because it determines the ethanolysis of the *MLn* tetrakis complex for Na, K, and Rb. In fact, *NaEu(+)* yields practically only the *tris* form $Eu(hfbc)_3$ in the few minutes necessary to sample preparation, and its ECD spectrum is almost equal to that of commercial $Eu(hfbc)_3$ (two very weak positive bands for *(+)-hfbc*); in addition, the couplet amplitudes for *KEu* and *RbEu* in $CHCl_3$−EtOH are the lowest ones, with respect to the other two solvents, while *CsEu* is almost equal for shape and intensity.
- In all these samples, we noticed the same precipitation phenomena discussed above, with Na > K > Rb; for dichloromethane and ethanol-stabilized chloroform, the absolute amounts of solid (starting from the same concentrations) are greater than for the amylene−chloroform solutions. [The spectra were always recorded on the clear part of the solution.]
- The ECD spectra for the *MEu(+)* complexes in amylene-stabilized chloroform immediately after dissolution undergo a time evolution: as shown in Figure S6 in the Supporting Information, for Na, K, and Rb, we observe the decrease of the couplet amplitude as a result of the formation of the *tris* complex, with rates that follow the order Na > K > Rb, in agreement with what we noticed for the ^{19}F NMR spectra. The *CsEu(+)* ECD spectrum remains unaltered, as expected.
- The "time zero" *MEu(+)* ECD spectra in amylene−chloroform, similar to the ^{19}F NMR spectra discussed above, contain the *tetrakis* species, prevalently, for each alkali-metal derivative. As a consequence, the different crossover points (λ_{zero} follows the order Na < K < Rb < Cs), the different couplet amplitudes, and the overall shape must be ascribed to slightly different solution structures, which may be the object of further study.

To conclude this section, we observe the following for $MLn(hfbc)_4$:

(1) The lighter alkali metal induces a higher propensity to decomposition to the *tris* complex $Ln(hfbc)_3$ (with the precipitation of M^+hfbc^-).
(2) $CsLn(hfbc)_4$ does not show any decomposition, neither with time nor with solvent composition.
(3) The geometry of the *tetrakis* species is affected, to some extent, by the size of M, as demonstrated by the (small) changes in the four spectroscopic parameters of the ECD spectra listed at the beginning of this section and by the ^1H-shifts (data not discussed in detail).

Because the focus of our work is on $CsLn(hfbc)_4$ and because the study of the complexes with other alkali metal in chloroform is complicated by the existence of the dissociation equilibrium, we did not further investigate the structural modifications induced by the different M-cations.

Geometrical Features of $CsEu(hfbc)_4$ and the Origin of Strong CPL. As we demonstrated above, these heterobimetallic compounds may undergo a more or less rich network of equilibria, depending on the alkali metal and the solvent. The only species that are stable and homogeneous in the series are

dx.doi.org/10.1021/ic3018979 | *Inorg. Chem.* 2012, 51, 12007−12014

the Cs compounds: *CsEu*, interestingly, also has the highest g_{lum} factor.

A first observation is that we deal with a robust coordination cage, providing eight coordination sites and precluding access to axial coordination, thanks to a small bite angle. This strong Cs−F bond survives in solution, even in the presence of polar protic solvents (EtOH), because of a good match between steric and electrostatic effects between the alkali ion and the perfluoroalkyl chains. Such a rigid environment and the absence of O−H oscillators around Eu^{3+} ensures good total luminescence.

The most remarkable aspect, however, consists of the fact that ∼85% of the emitted photons at ∼595 nm are left-circularly polarized (for *CsEu(+)*), and it would be extremely useful to ascertain which feature can be held mostly responsible for such a high discrimination.

The CPL intensity of a (electronic) transition a → b is related to the rotational strength, R_{ab}:

$$R_{ab} = \mathrm{Im}[\langle a|\boldsymbol{\mu}|b\rangle\cdot\langle b|\mathbf{m}|a\rangle] \quad (3)$$

where Im stands for the imaginary part, the dot represents the scalar product between the vector operators $\boldsymbol{\mu}$ and $\mathbf{m}$ denoting the electric and magnetic dipole moments, respectively. Intraconfigurational *f*−*f* transitions in lanthanides generally are electric dipole (Laporte) forbidden, because they occur among states of equal parity, which is true, in particular, for the $^5D_0 \rightarrow {}^7F_1$ of Eu^{3+} responsible for the 595-nm emission band. In order to gain rotational strength, it must acquire some electric dipole moment collinear with the magnetic one: following eq 1 and recalling that total absorption intensity is mostly due to the (electric) oscillator strength, one can derive the relation[25]

$$g_{ab} = 4\left(\frac{m_{ab}}{\mu_{ab}}\right)\cos\tau_{ab} \quad (4)$$

where m_{ab} and μ_{ab} represent the moduli of the terms in angular brackets in eq 3 and τ_{ab} the angle between the electric and magnetic dipole transition moments. In axial (presently, C_4) symmetry, τ_{ab} is necessarily 0°, 90°, or 180°, yielding positive, vanishing, or negative g_{ab} (and, equivalently, CPL signals).

Reference 25 provides theoretical insight into some of the factors determining CPL in Ln DOTA-like systems, whose square SAPR coordination cage is very similar to *CsLn(hfbc)*$_4$.

The focus of that analysis is on the cage provided by the first coordination sphere around the emitter, which is chiral only if the twist angle α (defined above and shown in Figure 2) is

$$\alpha \neq 0°, 45°$$

because the former value corresponds to a cubic coordination, the latter to a perfect square antiprism, which are both *locally achiral*. According to ref 25, the relative CPL should follow an equation

$$\mathrm{CPL} \approx \sin 2\alpha \cos 2\alpha \quad (5)$$

which, in DOTA-like Eu compounds, apparently leads to only modest values of g_{lum} (<0.3).

In the SAPR coordination of DOTA-like systems, the twist angle is approximated as

$$\alpha_{DOTA} = 40°$$

i.e., a value close to that presently found for *CsLn(hfbc)*$_4$ (as seen above, $\alpha = -41.4°$) and, accordingly, one may expect a grossly similar value of g_{lum}, which is clearly not the case.

The so-called *static coupling mechanism*,[26] which is implicit in the former analysis and is based only on the oxygen donor atoms of the Ln coordination sphere, is apparently insufficient to fully justify the extraordinary g_{lum} values of *CsEu* and *CsSm* and a further source of symmetry-breaking must be sought elsewhere. The next most obvious step is *dynamic coupling*[26,27] between Ln^{3+}-centered magnetic dipole transitions (Ln = Eu or Sm) and the polarizabilities brought about by the nearby and tightly bound diketonates through their $\pi-\pi^*$ transition at ∼310 nm.

At the origin of this mechanism, there is an electrostatic interaction between an electric multipole, associated to the lanthanide-centered magnetic transition (e.g., $^5D_0 \rightarrow {}^7F_1$ for Eu^{3+}), and ligand-centered electric dipoles $\boldsymbol{\mu}$. This perturbation element breaks the (almost-perfect) D_4 symmetry of the lanthanide chromophore only if $\boldsymbol{\mu}$ is skewed, with respect to the symmetry axis. This geometrical condition is exactly met presently, because the ligand-centered $\pi-\pi^*$ transition moment is oriented as the line joining the two O atoms. Following Figure 2, this is measured by the angle

$$\psi = -27.5°$$

This value (absolute value) is almost midway between the two achiral situations (ψ = 0°, 90°), whereby a value of $|\psi| = 45°$ would correspond to a maximum chirality.

Near-Infrared Electronic Circular Dichroism (NIR-ECD) of *CsYb*. As further, independent proof of the major role of dynamic coupling, compared to static coupling, we may consider the chiroptical properties of the extremely simple set of transitions provided by the $^2F_{7/2} \rightarrow {}^2F_{5/2}$ of the *CsYb* analogue.[28] Unlike that for most other Ln^{3+} species, this spectroscopic term is isolated and cannot borrow/lend rotational strength intraconfigurationally.

The NIR-ECD of *CsYb* is shown in Figure 5. It consists of a series of strongly overlapping bands, which are due to the crystal-field splitting (CFS) of the ground and excited states (which, for the isolated ion, would be 4- and 3-fold degenerate, respectively). [A further degeneracy arises from Kramers doublets due to Yb^{3+} paramagnetism. Because this is not lifted by CFS, it is ignored here.] Although it displays negative, as

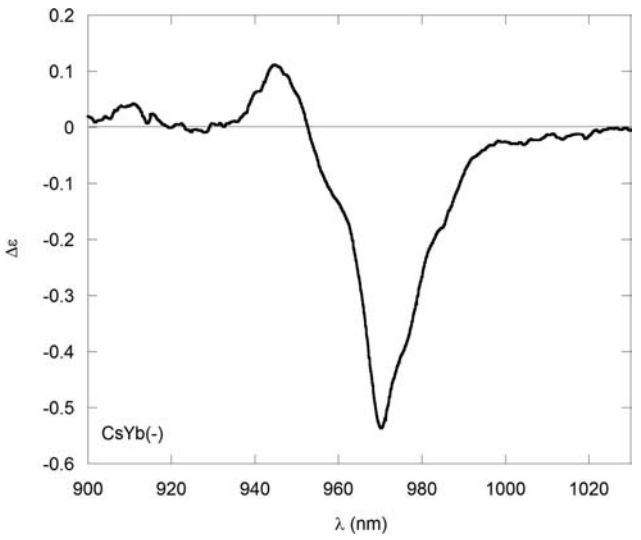

Figure 5. Near-infrared electronic circular dichroism (NIR-ECD) spectrum of the *CsYb(−)* complex (in $CHCl_3$).

dx.doi.org/10.1021/ic3018979 | *Inorg. Chem.* 2012, 51, 12007−12014

well as positive, signals, it is very clear that the *overall* rotational strength is nonvanishing (for *CsYb(−)*, it is negative): this is proof that this chiroptical property is not confined within the *f*-manifold but, rather, is due to a *coupling* involving other electronic transitions. The transition that is strongest and nearest in energy is the diketonate $\pi-\pi^*$ transition at ∼310 nm. Such an occurrence can be found in other Yb-complexes with achiral coordination polyhedra, but with dissymmetrically arranged ligands endowed with strong electric-dipole transitions.[29] In contrast, when the ligand is nonchromophoric, as it is in most Yb-DOTA derivatives,[30] or when the chromophore is remote from the lanthanide ion,[31−34] the NIR-ECD spectra display compensation of rotational strengths (this is also called a *conservative shape*).

Interestingly, one can make the same observation on the Eu^{3+} CPL spectra at ∼590 nm: when static coupling is dominant, the two bands of the $^5D_0 \rightarrow {}^7F_1$ transition are oppositely signed and compensate,[32] whereas in dynamic coupling, as in the present one and those listed in ref 4, there is a nonvanishing integral CPL at ∼595 nm.

CONCLUSION

CsEu provides the largest reported CPL dissymmetry factor (g_{lum} = 1.38), which implies that ∼85% of the emitted photons at 595 nm are left-circularly polarized.

The analysis of the paramagnetic NMR spectra reveals the isostructurality in solution across the series. We could accurately extract pseudo-contact shifts and relaxation rates and use them to determine a reliable solution structure, which displays an almost-perfect square antiprismatic Ln^{3+} coordination.

Apparently, Cs^+ fits in the cavity of perfluorinated chains very well and establishes strong binding interactions, preventing any dynamic rearrangement and providing a rigid structure, where the bite angle above the lanthanide ion is so small to prevent axial binding (e.g., to water). This aspect may concur in preventing Eu-luminescence quenching, frequently encountered in hydrated complexes.

The extraordinary value of g_{lum} cannot be due to the chirality of the coordination polyhedron, as tentatively suggested in the literature, but may be largely attributed to the dynamic coupling involving the diketonate $\pi-\pi^*$ transition. Indeed, the related dipoles display a skew angle of $|\psi|$ = 27°, with respect to the main symmetry axis, which is relatively close to the ideal value of 45° to induce maximum rotational strength and maximum polarized luminescence.

ASSOCIATED CONTENT

Supporting Information

Tables S1−S4 and Figures S1−S6. This material is available free of charge via the Internet at http://pubs.acs.org.

AUTHOR INFORMATION

Corresponding Author

*E-mail: ldb@dcci.unipi.it.

Notes

The authors declare no competing financial interest.

ACKNOWLEDGMENTS

Financial support from MIUR (Project No. 2009PRAM8L) is acknowledged. We are grateful to Dr. G. Pescitelli and Mr. C. Resta for stimulating discussions and help in the synthesis and measurements.

REFERENCES

(1) Muller, G. *Dalton Trans.* **2009**, 9692−9707.
(2) Riehl, J. P.; Muller, G. Circularly Polarized Luminescence Spectroscopy and Emission-Detected Circular Dichroism. In *Comprehensive Chiroptical Spectroscopy*; John Wiley & Sons, Inc.: New York, 2012; pp 65−90.
(3) Parker, D.; Dickins, R. S.; Puschmann, H.; Crossland, C.; Howard, J. A. K. *Chem. Rev.* **2002**, *102*, 1977−2010.
(4) Moore, E. G.; Samuel, A. P. S.; Raymond, K. N. *Acc. Chem. Res.* **2009**, *42*, 542−552.
(5) Other interesting cases can be found, e.g., in: (a) Harada, T.; Tsumatori, H.; Nishiyama, K.; Yuasa, J.; Hasegawa, Y.; Kawai, T. *Inorg. Chem.* **2012**, *51*, 6476−6485. (b) Samuel, A. P. S.; Lunkley, J. L.; Muller, G.; Raymond, K. N. *Eur. J. Inorg. Chem.* **2010**, 3343−3347. (c) Harada, T.; Nakano, Y.; Fujiki, M.; Naito, M.; Kawai, T.; Hasegawa, Y. *Inorg. Chem.* **2009**, *48*, 11242−11250. (d) Gregoliński, J.; Starynowicz, P. a.; Hua, K. T.; Lunkley, J. L.; Muller, G.; Lisowski, J. *J. Am. Chem. Soc.* **2008**, *130*, 17761−17773. (e) Seitz, M.; Moore, E. G.; Ingram, A. J.; Muller, G.; Raymond, K. N. *J. Am. Chem. Soc.* **2007**, *129*, 15468−15470. (f) Petoud, S.; Muller, G.; Moore, E. G.; Xu, J.; Sokolnicki, J.; Riehl, J. P.; Le, U. N.; Cohen, S. M.; Raymond, K. N. *J. Am. Chem. Soc.* **2006**, *129*, 77−83.
(6) Lunkley, J. L.; Shirotani, D.; Yamanari, K.; Kaizaki, S.; Muller, G. *J. Am. Chem. Soc.* **2008**, *130*, 13814−13815.
(7) Lunkley, J. L.; Shirotani, D.; Yamanari, K.; Kaizaki, S.; Muller, G. *Inorg. Chem.* **2011**, *50*, 12724−12732.
(8) Shirotani, D.; Suzuki, T.; Kaizaki, S. *Inorg. Chem.* **2006**, *45*, 6111−6113.
(9) Lin, Y.; Zou, F.; Wan, S.; Ouyang, J.; Lin, L.; Zhang, H. *Dalton Trans.* **2012**, *41*, 6696−6706.
(10) Shirotani, D.; Suzuki, T.; Yamanari, K.; Kaizaki, S. *J. Alloys Compd.* **2008**, *451*, 325−328.
(11) Bertini, I.; Luchinat, C. *Coord. Chem. Rev.* **1996**, 150.
(12) Piguet, C.; Geraldes, C. F. G. C. Paramagnetic NMR Lanthanide Induced Shifts for Extracting Solution Structures. In *Handbook on the Physics and Chemistry of Rare Earths*; Gschneidner, K. A., Jr.; Bunzli, J. C. G.; Pecharsky, V. K., Eds.; Elsevier: 2003; Vol. *33*, pp 353−463.
(13) Babailov, S. P. *Prog. Nucl. Magn. Reson. Spectrosc.* **2008**, *52*, 1−21.
(14) Di Bari, L.; Salvadori, P. *Coord. Chem. Rev.* **2005**, *249*, 2854−2879.
(15) Di Bari, L.; Salvadori, P. *ChemPhysChem* **2011**, *12*, 1490−1497.
(16) Ripoli, S.; Scarano, S.; Di Bari, L.; Salvadori, P. *Bioorg. Med. Chem.* **2005**, *13*, 5181−5188.
(17) Di Pietro, S.; Lo Piano, S.; Di Bari, L. *Coord. Chem. Rev.* **2011**, *255*, 2810−2820.
(18) Di Bari, L.; Pintacuda, G.; Ripoli, S.; Salvadori, P. *Magn. Reson. Chem.* **2002**, *40*, 396−405.
(19) Chin, K. O. A.; Morrow, J. R.; Lake, C. H.; Churchill, M. R. *Inorg. Chem.* **1994**, *33*, 656−664.
(20) Aime, S.; Botta, M.; Fasano, M.; Marques, M. P. M.; Geraldes, C. F. G. C.; Pubanz, D.; Merbach, A. E. *Inorg. Chem.* **1997**, *36*, 2059−2068.
(21) Richardson, M. F.; Wagner, W. F.; Sands, D. E. *J. Inorg. Nucl. Chem.* **1968**, *30*, 1275−1289.
(22) Wenzel, T. J.; Chisholm, C. D. *Prog. Nucl. Magn. Reson. Spectrosc.* **2009**, *59*, 1−63.
(23) Uccello-Barretta, G.; Balzano, F.; Salvadori, P. *Curr. Pharm. Des.* **2006**, *12*, 4023−4045.
(24) Berova, N.; Di Bari, L.; Pescitelli, G. *Chem. Soc. Rev.* **2007**, *36*, 914−931.
(25) Bruce, J. I.; Parker, D.; Lopinski, S.; Peacock, R. D. *Chirality* **2002**, *14*, 562−567.
(26) Richardson, F. S.; Faulkner, T. R. *J. Chem. Phys.* **1982**, *76*, 1595−1607.

(27) Mason, S. F. *Molecular Optical Activity and the Chiral Discriminations*; Cambridge University Press: Cambridge, U.K., 1982.
(28) Di Bari, L.; Salvadori, P. Chiroptical Properties of Lanthanide Compounds in an Extended Wavelength Range. In *Comprehensive Chiroptical Spectroscopy*; John Wiley & Sons, Inc.: New York, 2012; pp 221−246.
(29) Di Bari, L.; Lelli, M.; Pintacuda, G.; Pescitelli, G.; Marchetti, F.; Salvadori, P. *J. Am. Chem. Soc.* **2003**, *125*, 5549−5558.
(30) Di Bari, L.; Pescitelli, G.; Sherry, A. D.; Woods, M. *Inorg. Chem.* **2005**, *44*, 8391−8398.
(31) Dickins, R. S.; Howard, J. A. K.; Maupin, C. L.; Moloney, J. M.; Parker, D.; Riehl, J. P.; Siligardi, G.; Williams, J. A. G. *Chem.−Eur. J.* **1999**, *5*, 1095−1105.
(32) Maupin, C. L.; Dickins, R. S.; Govenlock, L. G.; Mathieu, C. E.; Parker, D.; Williams, J. A. G.; Riehl, J. P. *J. Phys. Chem. A* **2000**, *104*, 6709−6717.
(33) Di Bari, L.; Pintacuda, G.; Salvadori, P.; Dickins, R. S.; Parker, D. *J. Am. Chem. Soc.* **2000**, *122*, 9257−9264.
(34) Dickins, R. S.; Parker, D.; Bruce, J. I.; Tozer, D. J. *Dalton Trans.* **2003**, 1264−1271.

■ NOTE ADDED AFTER ASAP PUBLICATION

Due to a production error, this paper was published on the Web on October 24, 2012, without the Supporting Information. The corrected version was reposted on October 25, 2012.